

# PROBABILISTIC ANALYSIS OF DAILY RAINFALL IN SUMATRA RELATED TO ENSO AND IOD DYNAMICS DURING 1985–2023

Sudirman<sup>1</sup>, Hamdi Akhsan<sup>2</sup>, \*Muhammad Irfan<sup>3</sup>, Supari<sup>4</sup>, Suhadi<sup>5</sup>

<sup>1</sup>Doctoral of Mathematics and Natural Sciences, Universitas Sriwijaya, South Sumatra, Indonesia

<sup>1,2</sup>Physics Education, Universitas Sriwijaya, South Sumatra, Indonesia

<sup>3</sup>Physics, Universitas Sriwijaya, South Sumatra, Indonesia

<sup>4</sup>Indonesian Agency for Meteorological, Climatological and Geophysics, Jakarta, Indonesia

<sup>5</sup>Physics Education, Universitas Islam Negeri Raden Fatah, South Sumatra, Indonesia

\*Corresponding Author, Received: 07 Jan. 2026, Revised: 08 March 2026, Accepted: 10 March 2026

**ABSTRACT:** Sumatra lies between the Pacific and Indian Oceans, making its rainfall variability sensitive to large-scale ocean–atmosphere interactions like the El Niño–Southern Oscillation (ENSO) and Indian Ocean Dipole (IOD), based on observations from 19 stations of the Indonesian Agency for Meteorology, Climatology, and Geophysics. This study analyzed daily rainfall distribution in Sumatra during 1985–2023 using Probability Density Functions (PDF) for major seasons and ENSO and IOD phase classifications. La Niña and negative IOD enhanced atmospheric convergence and increased water vapor supply in western Indonesia, leading to more moderate to extreme rainfall events. In contrast, a positive El Niño–IOD combination is linked to dry conditions. Monte Carlo testing was conducted with 1000 resampling of neutral years to represent random distribution, testing if rainfall during ENSO/IOD phase differs from neutral conditions. Seasonal samples varied from 8 to 13 years per phase, with significance assessed using 5th and 95th percentiles. PDF analysis indicated a shift toward higher intensity during La Niña and negative IOD, with 18–27% of rainfall intensity bins surpassing the 95% confidence interval. During DJF season, several regions showed high-intensity rainfall frequencies during El Niño that exceeded the confidence interval, highlighting El Niño's role in regional extreme rainfall events. This pattern is explained by the dominance of westerly monsoon and regional convergence, which can modulate the classical ENSO signal. The findings confirmed that Sumatran rainfall response to ENSO–IOD interactions is seasonal, spatial, and nonlinear, with implications for understanding hydrometeorological risks in western Indonesia.

*Keywords: Rainfall, Variability, Climate, Extremes, Seasonality*

## 1. INTRODUCTION

Indonesia is an archipelagic country with a tropical climate characterized by high rainfall throughout the year, due to its location near the Equator, between the Asian and Australian continents, and bounded by the Pacific and Indian Oceans [1], [2]. Within this diverse climatic setting, the island of Sumatra, located along the western maritime continent and directly exposed to the Indian Ocean, represents one of the regions with pronounced rainfall variability influenced by both local and large-scale climate drivers [3], [4]. The island's complex topography, including the Barisan Mountain range, together with surrounding sea surface temperature (SST) variability, plays an important role in modulating cloud formation and precipitation patterns. Subyani et al. (2010) and et al. (2018) show that physical geographic conditions, including mountains, significantly influence rainfall distribution [5], [6]. Climatologically, Indonesia experiences four principal seasonal regimes: June–July–August (JJA), typically representing the dry season; September–October–November (SON), a transitional phase toward the wet season; December January–February (DJF), the peak rainy season

associated with the boreal winter monsoon; and March–April–May (MAM), a transition toward the subsequent dry season [7], [8]. Importantly, rainfall responses to ENSO and IOD exhibit marked seasonal dependence across these climatological periods. Climatologically, seasonal mean rainfall over Sumatra can vary by more than 50%–70% between the boreal winter wet season (DJF) and the boreal summer dry season (JJA), underscoring the strong seasonal modulation of hydroclimatic variability.

A substantial body of literature has established that ENSO and IOD are the main drivers of hydroclimate variability in Indonesia. Previous studies by Fadholi (2013) and Puryajati et al. (2021) demonstrated that ENSO significantly modulates Indonesian rainfall through alterations in tropical SST gradients and large-scale atmospheric circulation, particularly the Walker circulation [9], [10]. In Sumatra, the ENSO–rainfall relationship typically manifests as a moderate negative correlation (approximately  $-0.4$  to  $-0.6$ ), especially during SON, when enhanced Walker circulation anomalies amplify regional convective sensitivity to Pacific SST perturbations [11], [12]. Concurrently, the IOD, characterized by the zonal SST gradient between the western and eastern equatorial Indian Ocean, exerts a

substantial influence on regional precipitation. Positive IOD events are associated with rainfall reductions over Sumatra of approximately 20–40% relative to climatological means during JJA–SON, whereas negative IOD phases enhance convection and precipitation, particularly over western Sumatra [3], [7]. These findings underscore that the relationships among the Niño3.4 index, dipole mode index (DMI), and regional rainfall are inherently seasonal and nonlinear [11], [13]. These standardized classifications provide an objective framework for linking global climate variability modes to regional rainfall dynamics.

Despite extensive research on ENSO and IOD influences, most existing studies emphasize monthly or seasonal mean anomalies, thereby overlooking the full distributional characteristics of daily rainfall. Probabilistic analyses that explicitly examine changes in the entire rainfall distribution, particularly under the combined influence of ENSO and IOD across multiple seasons, remain limited, especially for Sumatra [14], [15]. This study addresses this gap by employing a probability density function (PDF) framework applied to daily rainfall observations from 1985 to 2023 at 19 Indonesian Agency for Meteorology, Climatology, and Geophysics (BMKG) stations across Sumatra [16]. The PDF approach enables a comprehensive assessment of distributional shifts, including changes in central tendency, skewness, and tail behavior, across the full spectrum of rainfall intensities. The generalized extreme value (GEV) framework, which primarily targets block maxima or peak-over-threshold extremes and is therefore inherently focused on upper-tail behavior [11], [17]. The PDF-based approach captures variability across low, moderate, and high rainfall intensities, which is an essential consideration in tropical precipitation systems, where moderate rainfall events contribute substantially to total accumulation and hydrological impacts [14], [15]. The statistical significance of distributional changes was evaluated using Monte Carlo resampling techniques, ensuring robust inference regarding the ENSO–IOD-related modulation of rainfall probabilities.

Given this background, there is a research gap regarding the lack of understanding of the probabilistic characteristics of daily rainfall in Sumatra in the context of cross-seasonal ENSO–IOD interactions. Specifically, the objectives of this study are to: (1) characterize the seasonal probabilistic distributions of daily rainfall across Sumatra for the period 1985–2023; (2) quantify the distributional responses of rainfall intensity to ENSO and IOD phases, both independently and in combination; and (3) identify statistically significant shifts in variability and occurrence probabilities across multiple rainfall

intensity classes using a PDF-based framework coupled with Monte Carlo significance testing. This paper is structured as follows. First, the research significance is elaborated to situate this study within rainfall-climate variability analysis in Sumatra. The study area, data sources, quality control procedures, ENSO and IOD phase classification, seasonal probability density function (PDF) construction, and Monte Carlo resampling framework for statistical significance testing are then described. The subsequent section presents and discusses the results, including data quality evaluation, identification of rainfall outliers, seasonal rainfall responses to ENSO and IOD, and their combined effects on rainfall variability. The paper concludes with a synthesis of findings and their implications for hydrometeorological risk assessment and climate adaptation strategies in Sumatra.

## **2. RESEARCH SIGNIFICANCE**

This study addresses a critical gap in rainfall–climate variability research in Sumatra by moving beyond trend analyses and mean-based anomaly assessments toward a distributional, daily-scale perspective. Although previous studies have explored rainfall trends, topographic controls, and large-scale circulation mechanisms, limited attention has been devoted to the probabilistic characteristics of daily rainfall in relation to ENSO and IOD across the four climatological seasons of JJA, SON, DJF, and MAM. By applying a PDF framework to long-term daily rainfall observations and standardized climate indices, this study provides a comprehensive evaluation of seasonal and combined ENSO–IOD effects on rainfall distributions. This approach offers a more refined understanding of hydroclimatic variability, thereby strengthening the scientific basis for climate impact assessment and water resource management in Sumatra.

## **3. METHODS**

Rainfall variability in Indonesia is influenced by global climate models, such as ENSO and IOD, as well as local factors, including topography and sea surface temperature. Climatologically, Indonesia experiences four seasonal regimes: DJF represents the rainy season, JJA represents the dry season, and MAM and SON represent transitional seasons. ENSO modulates rainfall through decreased rainfall during El Niño and increased rainfall during La Niña, whereas IOD primarily influences rainfall from June to November, with positive (negative) phases associated with decreased (increased) rainfall in Sumatra. The combined ENSO–IOD interaction can further intensify rainfall anomalies across Indonesia.



Fig.1 Location of the Indonesian Agency for Meteorology, Climatology, and Geophysics Stations.

### 3.1 Study Area and Rainfall Data

The data used in this study were obtained from the Indonesian Agency for Meteorology, Climatology, and Geophysics (BMKG), the official national provider of climate data in Indonesia. The study area covers Sumatra Island, one of Indonesia's largest islands, with a long mountainous topography known as the Barisan Mountains, extending from Aceh to Lampung, with maritime boundaries of the Bay of Bengal to the north, Sunda Strait to the south, Strait of Malacca to the east, and Indian Ocean to the west. Although the BMKG manages approximately 47 observation stations in Sumatra, most of these stations have relatively short rainfall recording periods, thus limiting data continuity. Therefore, this study used daily rainfall data from 19 BMKG stations with complete and continuous records from January 1, 1985, to the end of 2023. These stations were spread across 10 provinces, from Aceh Province in the north to Lampung Province in the south, with the largest concentrations of stations in Aceh Province and North Sumatra. The spatial distribution of these observation stations is shown in Fig. 1 (yellow triangles) and provides a solid basis for climatological analysis and the evaluation of rainfall variability in the Sumatra region.

### 3.2 Data Quality Control and Preparation

Figure 2 summarizes the overall theoretical–methodological workflow of this study. The daily rainfall dataset underwent quality control to ensure reliability prior to analysis. Missing values, including blank entries and coded values (e.g., 8888), were treated as missing data and excluded from the statistical calculations. Daily rainfall values equal to 0 mm were excluded from the rainfall–intensity PDF construction to ensure that the analysis represented

rainfall occurrence intensity rather than dry-day frequency. Data completeness was evaluated for each station, and stations with continuous records exceeding 80% completeness over 1985–2023 were retained. Outlier detection was performed using monthly and annual boxplots; however, extreme rainfall values were not automatically removed because they may represent physically valid events. Instead, suspicious values were cross-checked with neighboring stations and synoptic conditions, where available. The ENSO and IOD phases were classified using standardized thresholds. ENSO phases were defined using the Niño 3.4 index following the Oceanic Niño Index criterion: El Niño ( $\geq +0.5$  °C), La Niña ( $\leq -0.5$  °C), and neutral ( $-0.5$  °C < anomaly <  $+0.5$  °C). IOD phases were defined using the dipole mode index with thresholds of  $\geq +0.4$  °C (positive IOD),  $\leq -0.4$  °C (negative IOD), and neutral conditions between these limits. Years categorized as neutral simultaneously satisfied the neutral criteria for both indices and were used as the baseline population for subsequent statistical testing.

### 3.3 Seasonal PDF Construction

This study focuses on the statistical characterization of daily rainfall variability in Sumatra across the four climatological seasons (JJA, SON, DJF, and MAM) to evaluate distributional responses under ENSO and IOD climate states. Daily rainfall data were aggregated into climatological seasons (JJA, SON, DJF, and MAM). A sequential seasonal PDF analysis was performed. First, daily rainfall data were compiled according to each climatological season. Second, the maximum and minimum daily rainfall intensities were identified to determine the lower and upper bin limits for histogram construction. Third, rainfall-intensity distributions were estimated using a histogram-based

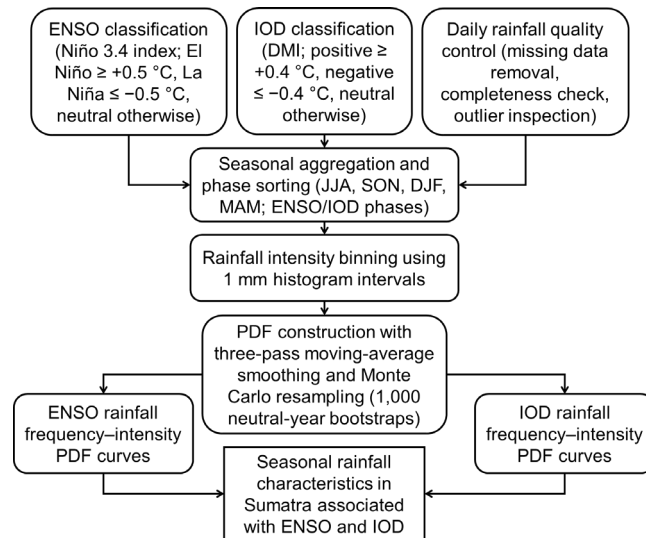


Fig.2 The theoretical-methodological workflow illustrating rainfall quality control, ENSO/IOD classification, neutral-year definition, histogram-based PDF construction with 1 mm bin width and smoothing, and Monte Carlo resampling (1,000 iterations) for significance assessment.

PDF approach with a fixed bin width of 1 mm spanning the observed rainfall range at each station. Fourth, frequency counts within each bin were converted into probabilities by dividing by the total number of rainfall occurrences. Fifth, the resulting probability series were smoothed using a three-point moving-average filter applied iteratively three times to reduce sampling noise while preserving the distribution shape. Sixth, seasonal PDF datasets corresponding to El Niño, La Niña, and neutral conditions were combined to enable a comparative analysis of rainfall distribution shifts across climate phases.

### 3.4 Monte Carlo Significance Testing

The statistical significance of ENSO- and IOD-related PDF anomalies was assessed using Monte Carlo resampling. A total of 1,000 bootstrap samples were generated by randomly selecting neutral-year rainfall records with replacement while preserving seasonal sample sizes. For each resample, PDFs were reconstructed using identical binning and smoothing procedures to form an empirical confidence envelope. The 5th and 95th percentiles of the Monte Carlo ensemble defined the two-sided 90% confidence interval. ENSO/IOD PDF curves exceeding this envelope were interpreted as statistically significant departures from neutral conditions. This Monte Carlo framework enables robust evaluation of rainfall distribution anomalies by accounting for sampling variability inherent in seasonal rainfall datasets.

### 3.5 Computational Implementation

All analytical procedures, including seasonal data aggregation, histogram-based PDF computation, smoothing operations, Monte Carlo resampling, and

frequency-rainfall curve generation, were implemented using Python within the Anaconda3 distribution and executed through Jupyter Notebook. Data directory configuration, workflow automation, and visualization routines were integrated into the computational pipeline to ensure the reproducibility and consistency of the results.

## 4. RESULTS AND DISCUSSION

### 4.1 Quality Assessment of Daily Rainfall Data

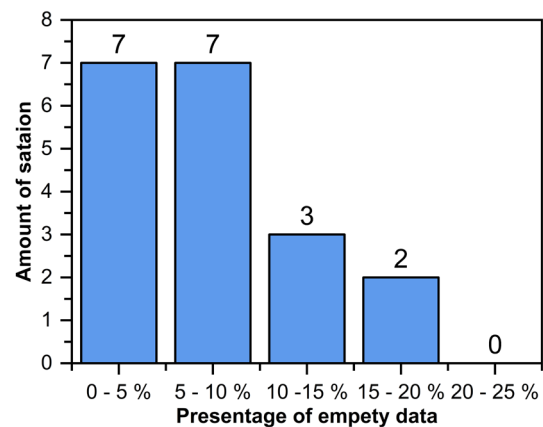


Fig.3 Daily rainfall data are unavailable.

The results of the first quality test on the percentage of daily rainfall data completeness at 19 research stations are shown in Fig.3. The quality The FL Tobing Station recorded the highest completeness (0.65%), whereas the Deli Serdang Meteorological Station in North Sumatra had the highest percentage of missing data at 18.70%, followed by the North Sumatra Meteorological Station (10.14%) and Radin Intan II (9.88%). Twelve stations fell into the very

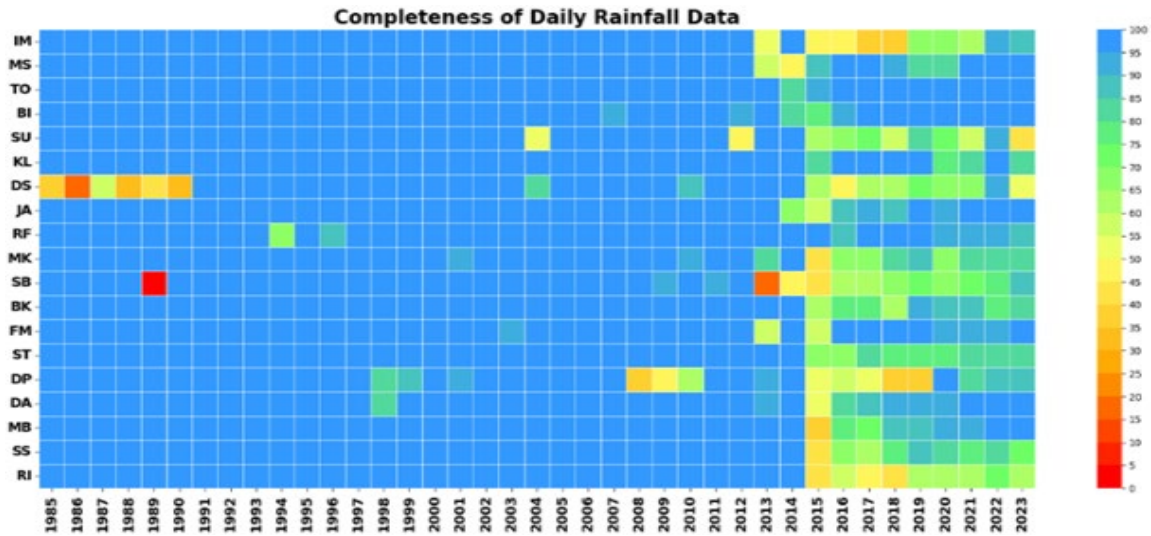


Fig.4 Percentage of completeness of daily rainfall data.

good category (0–5%), three stations into the good category (5–10%), and the remaining stations had completeness between 10% and 20%. The average completeness rate was 93%, and the dataset quality was deemed to meet the standards for a long-term climatological analysis.

The completeness of the daily rainfall data at most stations indicated high validity, as shown by the predominance of blue colors with average completeness levels of >93%. Some stations had periods of lower completeness: the Iskandar Muda Meteorological Station in 2015–2021 (>61%), Malikusaleh (2013–2014) Aceh, Deli Serdang Meteorological Station in North Sumatra (1985–1990; 2015–2021) ranging from 40% to 70%, Minangkabau Meteorological Station in West Sumatra (2013–2023) ranging from 50% to 80%, and West Sumatra Climatology Station (2014–2022) with 30%–70% completeness and total data gaps in 1989. The Bengkulu Climatology Station (2015–2018), Sultan Thaha and Depati Parbo Meteorological Stations, South Sumatra, and Radin Intan II (2015–2023) had completeness between 59% and 66%. The heatmap in Fig. 4 was used to visualize the data completeness in the dataset through visual quality checks of the complete (different colors), incomplete, and missing sections.

#### 4.2 Detection and Characteristics of Rainfall Outliers

The results of daily rainfall outlier detection were classified as follows: Based on the monthly boxplot analysis shown in Fig.5, the proportion of outlier data was less than 1%. At the FL Tobing Meteorological Station in North Sumatra, Minangkabau in West Sumatra, Fatmawati Soekarno in Bengkulu, the West Sumatra Climatology Station, and the Bengkulu Climatology Station, outliers occurred during the JJA (June – July – August) period

with very high daily rainfall intensity. Climatologically, this is unusual because the JJA is generally the dry season with low rainfall in Indonesia [11]. The FL Tobing station recorded three outliers of 300–430 mm/day, Minangkabau recorded seven outliers of 300–470 mm/day, the West Sumatra Climatology Station recorded six outliers of 300–320 mm/day, and two outliers each at Fatmawati Soekarno and Bengkulu Climatology (300–400 mm/day). Outliers >250 mm/day at the Raja Haji Fisabilillah Station in the Riau Islands remained consistent with the peak of the rainy season. Events exceeding 300 mm/day in June–July at several stations were considered abnormal as they did not correspond to the climatological conditions of the dry season. Spatially, extreme rainfall (>400 mm/day) is more dominant at Minangkabau, Fatmawati Soekarno, and Bengkulu Climatology Stations. The Aceh and Riau stations showed few outliers, and the southern Sumatra region was characterized by a lower frequency of outliers (150–265 mm/day). Spatial heterogeneity is influenced by the orography of the Bukit Barisan Mountains and proximity to the Indian Ocean and is consistent with projections of the lengthening dry season.

#### 4.3 Seasonal Rainfall Response to ENSO

During JJA, the El Niño effect on rainfall frequency was observed in the Aceh–Lampung region, particularly at low-to-moderate intensities, as shown in Fig.6. In Aceh, El Niño increases light-to-moderate rainy days compared to La Niña. Similar patterns occurred in North Sumatra, Riau, Jambi, South Sumatra, and Lampung, indicating that rainfall was not suppressed during El Niño. This demonstrated strong regional ENSO modulation. Lin et al., (2024) state that El Niño's impact on Southeast Asian rainfall is seasonal and regional, with positive rainfall anomalies occurring during dry seasons [18].

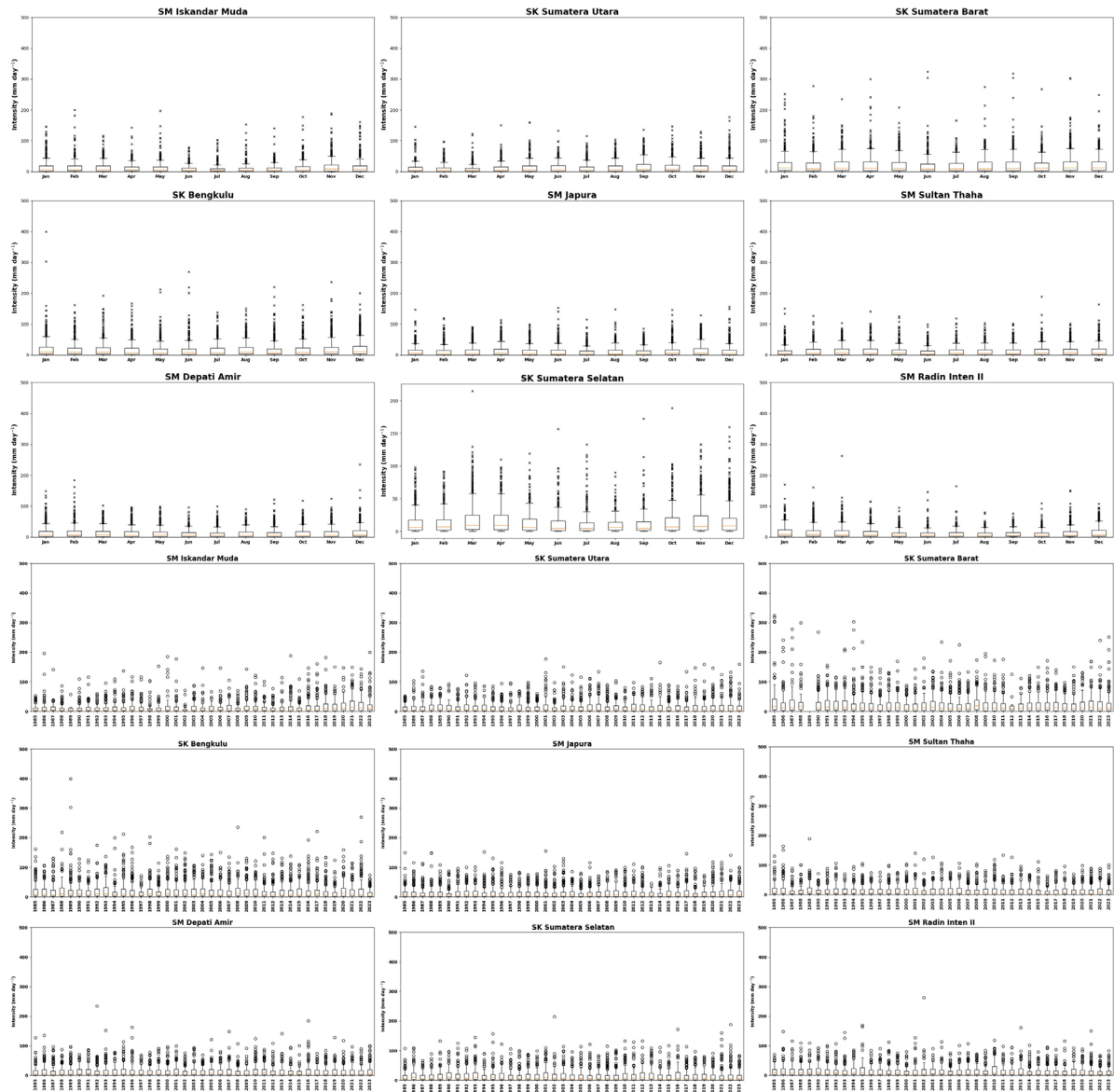


Fig.5 Boxplot of monthly-annual daily rainfall outliers.

Aldrian et al. (2011) noted that western Indonesia shows a different ENSO response, with rainfall continuing during the JJA [19], [20]. This study suggests that the impact of ENSO on rainfall extremes is non-stationary and dependent on the seasonal background [21]. During the SON season, the dominance shifted from El Niño to La Niña across the Aceh–Lampung region. Hendon et al, (2003) explains that La Niña enhances Walker circulation and water vapor supply during seasonal transitions[21]. Qian and Robertson (2010) found that ENSO's impact on rainfall depends on the season and regional circulation [22]. El Niño suppresses high-intensity events, while La Niña enhances convection and water vapor supply during transition toward monsoon peak.

The DJF season, representing the peak of the western monsoon ENSO response, exhibits a complex region-specific pattern. In Aceh and parts of North Sumatra,

El Niño often matches or exceeds La Niña at moderate to extreme intensities [21]. This diverges from the general ENSO pattern, indicating that during DJF, El Niño becomes a significant trigger for intense rainfall events. A similar pattern appeared in Jambi, South Sumatra, and Lampung, where the El Niño frequency often surpassed that of La Niña at high intensities. These patterns indicate that western monsoon and regional atmospheric dynamics mask or reverse the classic ENSO signal during the peak rainy season. During DJF, El Niño and La Niña differences in extreme rainfall become less distinct to owing an monsoon dominance [19], [23]. In the MAM season, rainfall intensity shows the highest variability and the most heterogeneous ENSO response along the Aceh–Lampung. In Aceh, La Niña dominated, with a higher frequency across the moderate-to-high intensity range. La Niña strengthens the Walker Circulation and moisture supply during the transition season [24].

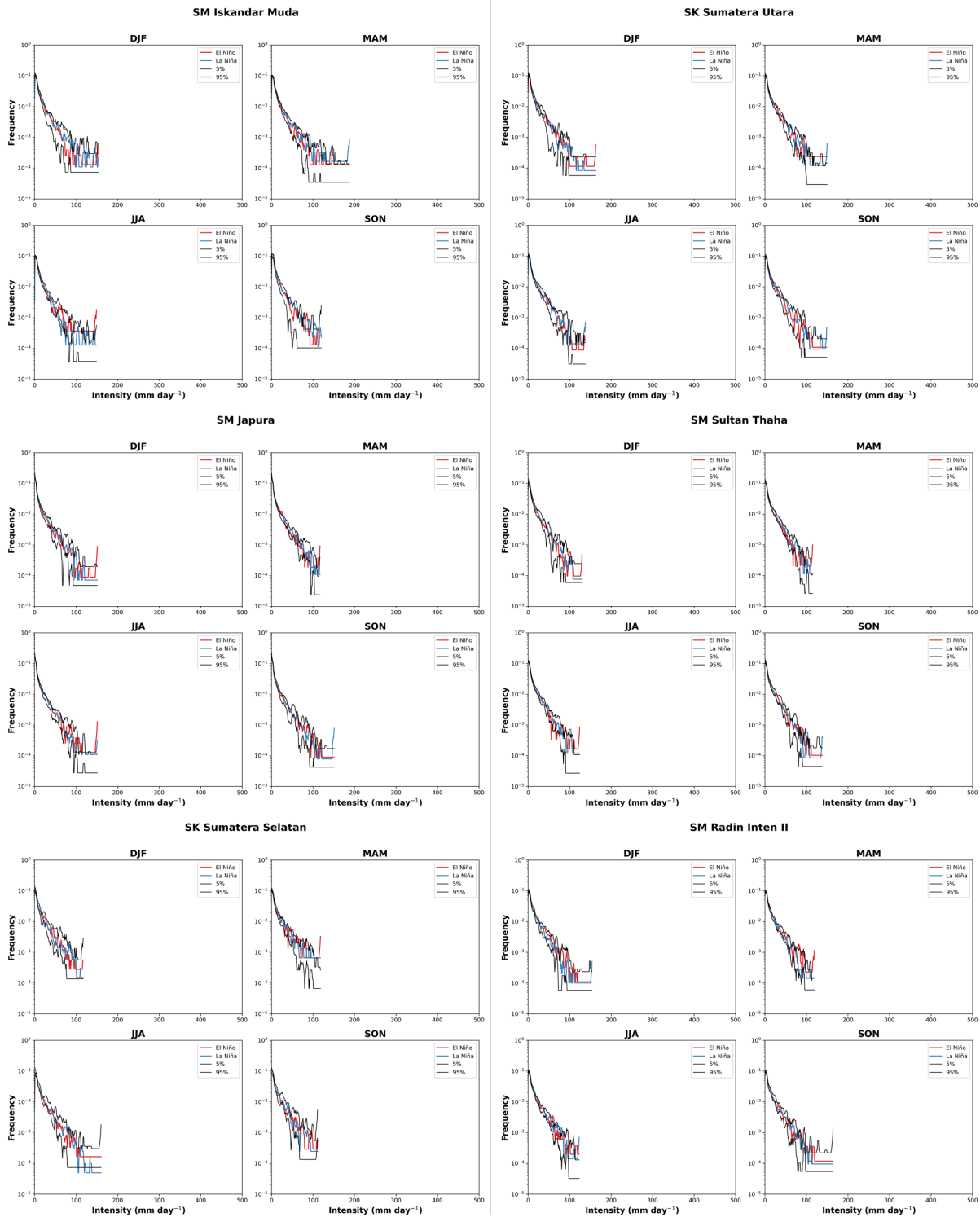


Fig.6 PDF of ENSO Aceh (SK Iskandar Muda), North Sumatra (SK Sumatera Utara), Riau (SM Japura), Jambi (SM Sultan Thaha), South Sumatra (SK Sumatera Selatan) and Lampung (SM Raden Inten II).

In Riau, Jambi, South Sumatra, and Lampung, El Niño showed a significant anomaly pattern in moderate-to-high rainfall frequency. MAM represents complex interactions between ENSO, monsoons, and local factors. The ENSO's impact on rainfall risk is not spatially uniform and requires seasonal analysis [25]. During the DJF and MAM

seasons, the ENSO–rainfall correlation in many Indonesian regions becomes insignificant.

#### 4.4 Seasonal Rainfall Response to IOD

During the JJA season, the rainfall response to IOD in Aceh–Lampung showed a clear spatial gradient. On the coasts of Aceh and western Sumatra,

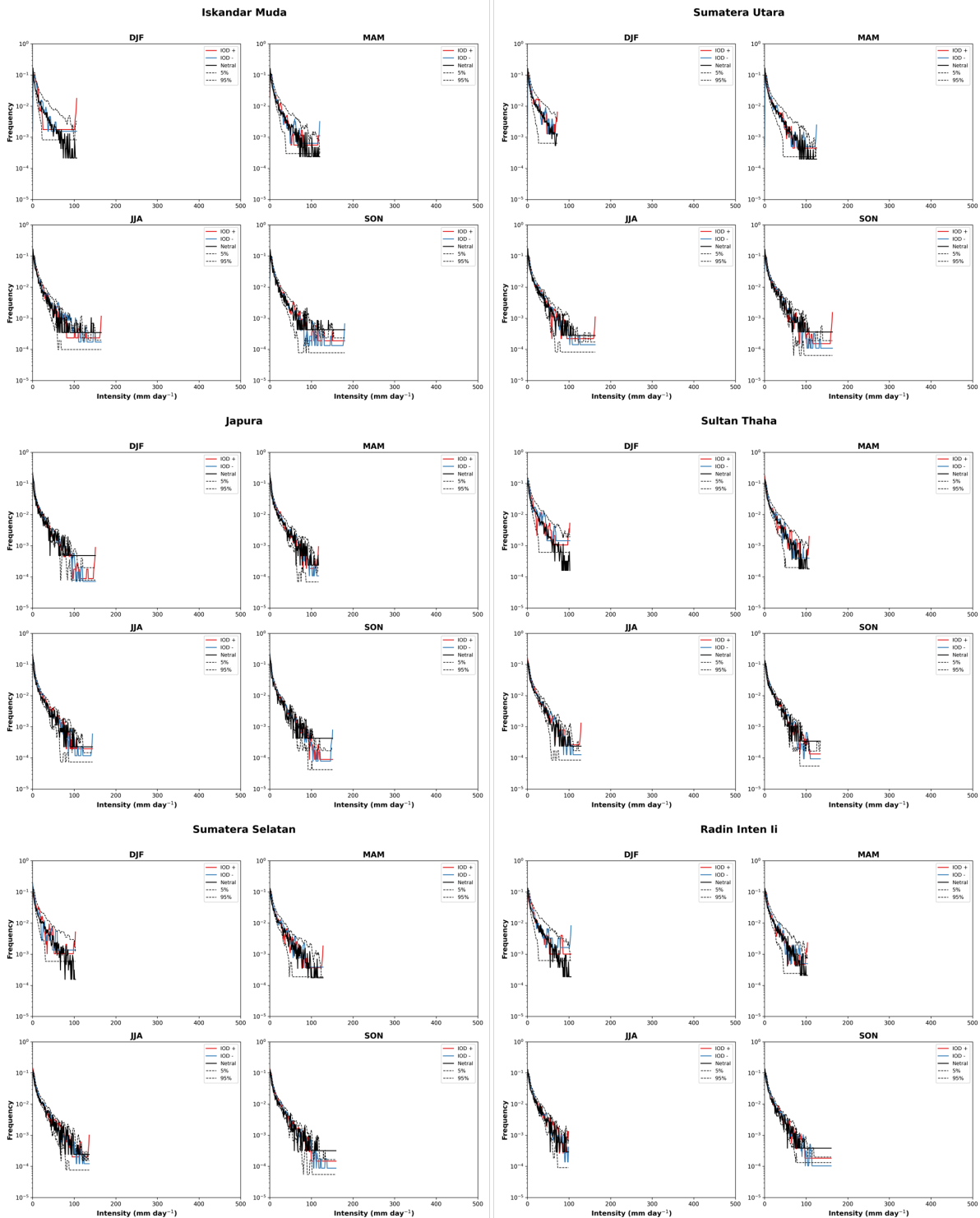


Fig.7 PDF of IOD Aceh (Iskandar Muda), North Sumatra (Sumatera Utara), Riau (SM Japura), Jambi (Sultan Thaha), South Sumatra (Sumatera Selatan) and Lampung (Raden Inten II).

negative IOD increases low–medium intensity rainfall frequency, as shown in Fig.7. SST warming in the eastern Indian Ocean strengthens regional convection. A positive IOD suppresses rainfall frequency in the medium–high-intensity class [14], [20]. However, sporadic extreme events have occurred at several locations. Low rainfall in South Sumatra during July–October is caused by a positive

IOD [26]. In Riau, Jambi, and Lampung, positive IOD dominated at medium–extreme intensity during the dry season. Although less frequent, positive IOD can increase heavy rainfall through regional convergence mechanisms and local dynamics. During JJA, a positive IOD typically suppresses convection in southern Indonesia. A negative IOD increases SST in the eastern Indian Ocean and supports moist

convection[26], [27]. During SON, negative IOD dominance became consistent in Aceh. West Sumatra experiences higher medium–high-intensity rainfall compared to positive IOD. Iskandar et.al (2022) state that negative IOD increases heavy rainfall on the west coast of Sumatra [28]. The negative SST anomaly in the eastern Indian Ocean supported an increased water vapor supply and convection over Sumatra. In central and southern Sumatra to Lampung, positive IOD shows a higher frequency of heavy–extreme rainfall intensity. These contrasting patterns show that the influence of IOD varies by geographical position. Eastern Sumatra responds to atmospheric anomalies with positive IOD. Cai & Cowan, (2013) stated that IOD effectively modulates extreme rainfall during dry and transitional seasons [29].

Southern Sumatra experiences rainy and dry seasons annually, which are related to changing monsoon winds[30], [31]. During DJF, which marks the peak of the wet monsoon, rainfall frequency differences between positive and negative IOD phases weaken at low-moderate intensities owing to monsoon system dominance. Suhadi et al., (2023) reported negative IOD remains associated with increased extreme rainfall during DJF, though the signal weakens [32]. At high-extreme intensities, negative IOD showed greater frequency in Aceh, South Sumatra, Jambi, and Lampung. This aligns with negative IOD, which strengthens upwelling and increases water vapor in western Indonesia. In some locations, extreme events during positive IOD continue, indicating local modulation over seasonal monsoon transition[33]. Consistent with Kajita et al., (2022), this emphasizes the IOD-monsoon interaction in triggering regional extreme rainfall [34]. A negative IOD increases the spatial variability of monsoon rainfall. A positive IOD reduces rainfall in several areas. During the MAM period, the rainfall response to IOD becomes the most heterogeneous and weakens. Negative IOD increases the moderate-to-high rainfall frequency in Aceh and western Sumatra. In central-southern Sumatra, including Lampung, the response differences between the IOD phases decreased [35]. The extreme rainfall response intensities intersect, indicating a weakened IOD influence during the transition season. This indicates the dominance of other factors, such as the MJO, local variability, and regional monsoon dynamics.

#### **4.5 Combined Effects of ENSO and IOD on Rainfall Variability**

During the JJA season, ENSO and IOD phenomena strongly influence the amplitude, duration, intensity, and frequency of average and extreme rainfall [36]. El Niño, often with positive IOD, suppresses light to moderate rainfall in Aceh and western Sumatra due to weakened convection and reduced moisture from the eastern Indian Ocean [35].

La Niña and/or negative IOD increases light to moderate rainfall over Aceh to Lampung, indicating strengthened convection from warm SST anomalies in the eastern Indian Ocean and western Pacific. ENSO and IOD modulate the variability of monsoon rainfall state that global SST anomalies modulate extreme rainfall in Southeast Asia through monsoon circulation and regional convective processes [37]. El Niño and positive IOD associate with drier conditions, while La Niña increases extreme rainfall[38]. The moderate and strong positive IOD events of 2019 and 2023 caused numerous disasters in Southeast Asia [39].

The combined influence of ENSO and IOD on rainfall in Sumatra during the SON and MAM seasons is spatially complex. The combination of negative IOD and La Niña increases the frequency of moderate to heavy rainfall[40] through strengthened lower-layer convergence, convective activity, and moisture transport into western Indonesia, Aceh, West Sumatra, and Southeast South Sumatra [37], [38]. In Lampung, Riau, and Bangka Belitung, positive IOD correlates with higher extreme rainfall, indicating regional mechanisms and MJO interactions in the region. In the DJF season, Asian monsoon dominance weakens the ENSO–IOD influence [40], [41]. La Niña–negative IOD increases moderate to extreme rainfall frequency from Aceh to Lampung. The ENSO–IOD influence on rainfall is stronger in the dry season (JJA-SON) than in the wet season (DJF) [42], [43]. These results show that hydrometeorological risks in Sumatra depend on seasonal ENSO–IOD interactions and regional conditions, affecting forest fire mitigation and peatland management on Sumatra's eastern coast.

#### **5. CONCLUSIONS**

This study provides a comprehensive probabilistic evaluation of daily rainfall variability across Sumatra and demonstrates that rainfall responses to ENSO and IOD are strongly seasonal, spatially heterogeneous, and nonlinear. The results show that La Niña consistently enhances the frequency of moderate-to-extreme rainfall events, particularly during SON and MAM, reflecting strengthened moisture transport and atmospheric convergence over western Indonesia. However, during DJF, when the Asian monsoon reaches its peak, ENSO signals become more complex and regionally modulated. In several areas, such as Aceh and Riau, El Niño does not simply suppress rainfall but can coincide with elevated extreme rainfall frequencies under strong monsoonal and regional convergence influences. During JJA, El Niño tends to increase light-to-moderate rainfall frequencies, while extreme rainfall remains limited, indicating that ENSO impacts cannot be interpreted using a simple wet-versus-dry framework. The influence of IOD is

most pronounced during JJA–SON, when negative IOD phases enhance moderate-to-high rainfall over western coastal Sumatra due to warming in the eastern Indian Ocean and intensified convection. Conversely, positive IOD phases, although typically associated with drier regional conditions, may increase localized extreme rainfall in central and eastern Sumatra during JJA and MAM when interacting with regional atmospheric dynamics. During DJF, IOD-related contrasts weaken due to dominant monsoon forcing. Overall, the findings confirm that rainfall anomalies in Sumatra result from the combined modulation of ENSO, IOD, seasonal monsoon circulation, and regional ocean–atmosphere interactions. These results have important practical implications. For early warning systems, seasonal forecasts should simultaneously incorporate ENSO and IOD phases rather than relying solely on ENSO classification, especially to anticipate heightened flood risk during La Niña–negative IOD conditions in SON and MAM and potential extreme rainfall during El Niño in DJF. In water resource management, reservoir operation, irrigation planning, and watershed management strategies should adopt season-specific probabilistic rainfall information to balance flood control and drought mitigation. For agriculture, particularly rain-fed systems, integrating seasonal climate phase information can reduce crop losses by optimizing planting calendars and improving preparedness for excessive rainfall or drought. Moreover, peatland and forest fire management in eastern Sumatra would benefit from improved drought anticipation during El Niño–positive IOD conditions in the dry season. Therefore, hydrometeorological risk assessment and climate adaptation planning in Sumatra must be based on an integrated, seasonally resolved climate framework that accounts for the interactive effects of ENSO, IOD, and regional dynamics rather than a single large-scale climate indicator.

## 6. REFERENCES

1. Vinata R.T., Kumala M.T., and Serfiyani C.Y., Climate change and reconstruction of Indonesia's geographic basepoints: Reconfiguration of baselines and Indonesian Archipelagic Sea lanes, *Marine Policy*, Vol.148, 2023, p.105443. <https://doi.org/10.1016/j.marpol.2022.105443>
2. Munawar M., Prasetya T.A.E., McNeil R., Jani R., and Buya S., Spatio and Temporal Analysis of Indonesia Land Surface Temperature Variation During 2001–2020, *Journal of the Indian Society of Remote Sensing*, Vol.51, No.7, 2023, pp.1393-1407. <https://doi.org/10.1007/s12524-023-01713-0>
3. Rachman H.A. et al., Dynamic of upwelling variability in southern Indonesia region revealed from satellite data: Role of ENSO and IOD, *Journal of Sea Research*, Vol.202, 2024, p.102543. <https://doi.org/10.1016/j.seares.2024.102543>
4. Yulianti K.K., Ningsih N.S., Rachmayani R., and Prasetyo E., The influence of El Niño–Southern Oscillation (ENSO) on the characteristics of tropical cyclones in Indonesia waters, *Tropical Cyclone Research and Review*, Vol.14, No.3, 2025, pp.270-286. <https://doi.org/10.1016/j.tcr.2025.08.002>
5. Subyani A.M., Al-Modayan A.A., and Al-Ahmadi F.S., Topographic, seasonal and aridity influences on rainfall variability in western Saudi Arabia, *Journal of Environmental Hydrology*, Vol.18, No.2, 2010, pp.1-11.
6. Prasetyo B., Irwandi H., and Pusparini N., Karakteristik Curah Hujan Berdasarkan Ragam Topografi Di Sumatera Utara, *Jurnal Sains dan Teknologi Modifikasi Cuaca*, Vol.19, No.1, 2018, pp.11-18. <https://doi.org/10.29122/jstmc.v19i1.2787>
7. Tian X., Tang C., Wu X., Yang J., Zhao F., and Liu D., The global spatial-temporal distribution and EOF analysis of AOD based on MODIS data during 2003–2021, *Atmospheric Environment*, Vol.302, 2023. <https://doi.org/10.1016/j.atmosenv.2023.119722>
8. Boyaj A. and Vijayaraghavan S., Quantifying long-term variability and extremes in Southeast Asia's rainfall: a 40-year observational study (1980–2019), *Theoretical and Applied Climatology*, Vol.156, No.7, 2025. <https://doi.org/10.1007/s00704-025-05655-0>
9. Fadholi A., Pemanfaatan Suhu Udara dan Kelembaban Udara dalam Persamaan Regresi untuk Simulasi Prediksi Total Hujan Bulanan di Pangkalpinang, *CAUCHY: Jurnal Matematika Murni dan Aplikasi*, Vol.3, No.1, 2013, pp.1-9. <https://doi.org/10.18860/ca.v3i1.2565>
10. Puryajati A.D. et al., The Effect of ENSO and IOD on the Variability of Sea Surface Temperature and Rainfall in the Natuna Sea, *IOP Conference Series: Earth and Environmental Science*, Vol.750, No.1, 2021, pp.1-12. <https://doi.org/10.1088/1755-1315/750/1/012020>
11. Harapan H. et al., Effects of El Niño Southern Oscillation and Dipole mode index on Chikungunya infection in Indonesia, *Tropical Medicine and Infectious Disease*, Vol.5, No.3, 2020. <https://doi.org/10.3390/tropicalmed5030119>
12. Irfan M., Safrina S., Awaluddin, Sulaiman A., Virgo F., and Iskandar I., Analysis of rainfall and temperature dynamics in peatlands during 2018-2021 climate change, *International Journal of GEOMATE*, Vol.23, No.99, 2022. <https://doi.org/10.21660/2022.99.3562>

13. Mulsandi A., Koesmaryono Y., Hidayat R., Faqih A., and Sopaheluwakan A., On the interannual variability of Indonesian Monsoon Rainfall (IMR): A literature review of the role of its external forcing, *Jurnal Meteorologi dan Geofisika*, Vol.24, No.2, 2024, pp.115-127. <https://doi.org/10.31172/jmg.v24i2.1049>
14. Afifah Azuga N. and Habibullah A.D., Interannual variability of sea level anomaly (SLA) in the western Sumatra coastal waters driven by ENSO and IOD modulations, *Asian Journal of Aquatic Sciences*, Vol.7, No.3, 2024. <https://doi.org/10.31258/ajoas.7.3.422-431>
15. Nurdiati S., Sopaheluwakan A., and Septiawan P., Joint distribution analysis of forest fires and precipitation in response to ENSO, IOD, and MJO (Study case: Sumatra, Indonesia), *Atmosphere*, Vol.13, No.4, 2022. <https://doi.org/10.3390/atmos13040537>
16. Shi W. and Wang M., Biological dipole mode indices: New parameters to characterize the physical and biological processes of the Indian Ocean Dipole event, *Progress in Oceanography*, Vol.206, 2022. <https://doi.org/10.1016/j.pocean.2022.102847>
17. Sireesha P.V. and Sandhya T., Statistical analysis of wind power density using different mixture probability distribution functions in coastal region of Andhra Pradesh, *Electrical Engineering*, Vol.106, No.3, 2024. <https://doi.org/10.1007/s00202-023-02104-x>
18. Lin S., Dong B., Yang S., He S., and Hu Y., Causes of diverse impacts of ENSO on the Southeast Asian summer monsoon among CMIP6 models, *Journal of Climate*, Vol.37, No.2, 2024, pp.419-438. <https://doi.org/10.1175/JCLI-D-23-0303.1>
19. Krishnan A., Bhaskaran P.K., and Kumar P., Extreme wind-wave climate projections for the Indian Ocean under changing climate scenarios, *Climate Dynamics*, Vol.59, No.3-4, 2022. <https://doi.org/10.1007/s00382-022-06147-x>
20. Wandayantolis W., Budianta D., and Gunawan D., Investigating the impacts of ENSO and IOD on rice productivity in South Sumatra, Indonesia, *Proceedings of the 10th International Conference on Agriculture*, Vol.8, No.1, 2023. <https://doi.org/10.17501/26827018.2023.8103>
21. Hendon H.H., Indonesian rainfall variability: Impacts of ENSO and local air-sea interaction, *Journal of Climate*, Vol.16, No.11, 2003, pp.1775-1790. <https://doi.org/10.1175/1520-0442>
22. Qian J.H., Robertson A.W., and Moron V., Interactions among ENSO, the Monsoon, and Diurnal Cycle in Rainfall Variability over Java, Indonesia, *Journal of the Atmospheric Sciences*, Vol.67, No.11, 2010, pp.3509-3524. <https://doi.org/10.1175/2010JAS3348.1>
23. Najibi N., Mazor A., Devineni N., Mossel C., and Booth J.F., Understanding the spatial organization of simultaneous heavy precipitation events over the conterminous United States, *Journal of Geophysical Research: Atmospheres*, Vol.125, No.23, 2020. <https://doi.org/10.1029/2020JD033036>
24. Rodysill J.R., Russell J.M., Vuille M., Dee S., Lughino B., and Bijaksana S., La Niña-driven flooding in the Indo-Pacific warm pool during the past millennium, *Quaternary Science Reviews*, Vol.225, 2019. <https://doi.org/10.1016/j.quascirev.2019.106020>
25. Putri Maulida N., Ariska M., Suhadi, and Akhsan H., Rainfall characteristics in Kalimantan Island during ENSO and IOD phases: Insights from composite analysis, *Jurnal Ilmu Fisika*, Vol.17, No.1, 2025. <https://doi.org/10.25077/jif.17.1.88-100.2025>
26. Irfan M., Safrina S., Koriyanti E., Kurniawati N., Saleh K., and Iskandar I., Effects of climate anomaly on rainfall, groundwater depth, and soil moisture on peatlands in South Sumatra, Indonesia, *Journal of Groundwater Science and Engineering*, Vol.11, No.1, 2023, pp.81-88. <https://doi.org/10.26599/JGSE.2023.9280008>
27. Lestari D.O., Sutriyono E., Kadir S., and Iskandar I., Impact of 2016 weak La Niña Modoki event over the Indonesian region, *International Journal of GEOMATE*, Vol.17, No.61, 2019. <https://doi.org/10.21660/2019.61.8256>
28. Iskandar I. et al., Extreme Positive Indian Ocean Dipole in 2019 and Its Impact on Indonesia, *Sustainability*, Vol.14, No.22, 2022, pp.1-15. <https://doi.org/10.3390/su142215155>
29. Cai W. and Cowan T., Southeast Australia autumn rainfall reduction: A climate-change-induced poleward shift of ocean-atmosphere circulation, *Journal of Climate*, Vol.26, No.1, 2013, pp.189-205. <https://doi.org/10.1175/JCLI-D-12-00035.1>
30. Mardiansyah W., Setiabudidaya D., Khakim M.Y.N., Yustian I., Dahlan Z., and Iskandar I., On the influence of ENSO and IOD on rainfall variability over the Musi Basin, South Sumatra, *Science and Technology Indonesia*, Vol.3, No.4, 2018, pp.157-163. <https://doi.org/10.26554/sti.2018.3.4.157-163>
31. Affandi A.K., Safrina S., Awaluddin, Sulaiman A., and Irfan M., Effect of climate anomaly in 2023 dry season on rainfall, groundwater level, soil moisture and hotspot on peatlands, *International Journal of GEOMATE*, Vol.28, No.127, 2025. <https://doi.org/10.21660/2025.127.4797>
32. Suhadi, Iskandar I., Supari, Irfan M., and Akhsan H., Extreme drought assessment in Sumatra-Indonesia using SPI and EDI, *Science*

- and Technology Indonesia, Vol.8, No.4, 2023, pp.691-700. <https://doi.org/10.26554/sti.2023.8.4.691-700>
33. Jain S., Turkington T., Tan W.L., Schwartz C., Scaife A.A., and Shepherd T.G., Towards developing an operational Indian Ocean Dipole warning system for Southeast Asia, *Scientific Reports*, Vol.15, No.1, 2025, pp.1-12. <https://doi.org/10.1038/s41598-025-99261-9>
34. Kajita R., Yamanaka M.D., and Kozan O., Reconstruction of rainfall records at 24 observation stations in Sumatera, Colonial Indonesia, from 1879 to 1900, *Journal of Hydrometeorology*, Vol.23, No.10, 2022, pp.1627-1643. <https://doi.org/10.1175/JHM-D-20-0245.1>
35. Kisakye V. and Van der Bruggen B., Effects of climate change on water savings and water security from rainwater harvesting systems, *Resources, Conservation and Recycling*, Vol.138, 2018. <https://doi.org/10.1016/j.resconrec.2018.07.009>
36. Mardiansyah W., Setiabudidaya D., Khakim M.Y.N., Yustian I., Dahlan Z., and Iskandar I., On the influence of ENSO and IOD on rainfall variability over the Musi Basin, South Sumatra, *Science and Technology Indonesia*, Vol.3, No.4, 2018, pp.157-163. <https://doi.org/10.26554/sti.2018.3.4.157-163>
37. Hidayat R. and Ando K., Variabilitas Curah Hujan Indonesia dan Hubungannya dengan ENSO/IOD: Estimasi Menggunakan Data JRA-25/JCDAS, *Agromet*, Vol.28, No.1, 2018, pp.1-8. <https://doi.org/10.29244/j.agromet.28.1.1-8>
38. Supari, Tangang F., Salimun E., Aldrian E., Sopaheluwakan A., and Juneng L., ENSO modulation of seasonal rainfall and extremes in Indonesia, *Climate Dynamics*, Vol.51, No.7-8, 2018, pp.2559-2580. <https://doi.org/10.1007/s00382-017-4028-8>
39. Jain S., Turkington T., Tan W.L., Schwartz C., Scaife A.A., and Shepherd T.G., Towards developing an operational Indian Ocean Dipole warning system for Southeast Asia, *Scientific Reports*, Vol.15, No.1, 2025, pp.1-12. <https://doi.org/10.1038/s41598-025-99261-9>
40. Kurniadi A., Weller E., Min S.K., and Seong M.G., Independent ENSO and IOD impacts on rainfall extremes over Indonesia, *International Journal of Climatology*, Vol.41, No.6, 2021, pp.3640-3656. <https://doi.org/10.1002/joc.7040>
41. Narulita I., Pengaruh ENSO dan IOD pada Variabilitas Curah Hujan di DAS Cerucuk, Pulau Belitung, *Jurnal Tanah dan Iklim*, Vol.41, No.1, 2017, pp.45-60.
42. Suhadi, Iskandar I., Supari, Irfan M., and Akhsan H., Extreme drought assessment in Sumatra-Indonesia using SPI and EDI, *Science and Technology Indonesia*, Vol.8, No.4, 2023, pp.691-700. <https://doi.org/10.26554/sti.2023.8.4.691-700>
43. Prasetyo L.B. et al., Assessing Sumatran peat vulnerability to fire under various condition of ENSO phases using machine learning approaches, *Forests*, Vol.13, No.6, 2022, p.828. <https://doi.org/10.3390/f13060828>

---

Copyright © Int. J. of GEOMATE All rights reserved, including making copies, unless permission is obtained from the copyright proprietors.

---